INSTITUTE OF PHYSICS PUBLISHING SUPERCONDUCTOR SCIENCE AND TECHNOLOGY
Supercond. Sci. Technol. **19** (2006) 96–101 doi:10.1088/0953-2048/19/1/016

In situ investigations of phase transformations in Fe-sheathed MgB_2 wires

J-C Grivel[1], R Pinholt[1], N H Andersen[1], P Kováč[2], I Hušek[2] and J Homeyer[3]

[1] Materials Research Department, Risø National Laboratory, Frederiksborgvej 399, 4000 Roskilde, Denmark
[2] Institute of Electrical Engineering, Slovak Academy of Sciences, Dúbravska cesta 9, 842 39 Bratislava, Slovakia
[3] Hamburger Synchrotronstrahlungslabor, Deutsches Elektronen-Synchrotron, Notkestrasse 85, 22603 Hamburg, Germany

Received 1 September 2005, in final form 9 November 2005
Published 6 December 2005
Online at stacks.iop.org/SUST/19/96

Abstract
The phase evolution inside Fe-sheathed wires containing precursor powders consisting of a mixture of Mg and B has been studied *in situ* by means of x-ray diffraction with hard synchrotron radiation (90 keV). Mg was found to disappear progressively during the heating stage. At 500 °C, the intensity of the Mg diffraction lines is reduced by about 20%. This effect is partly attributable to MgO formation. The MgB_2 phase was detected from 575 °C. Fe_2B was forming at the interface between the sheath and the ceramic core at sintering temperatures of 780 and 700 °C, but not at 650 °C. The formation rate of this phase is strongly dependent on the heat treatment temperature. Its presence can be readily detected as soon as the average interface reaction thickness exceeds 150–200 nm.

1. Introduction

The discovery of superconductivity in MgB_2 [1] resulted in a tremendous activity in the development of superconducting wires and tapes based on this promising material [2–9]. In spite of very encouraging early results, improvements of the critical current density, irreversibility field and thermal stability are still required before MgB_2-based conductors can become a viable alternative to superconducting wires and tapes based on other materials [10]. To reach this objective, an in-depth understanding of the interplay between the processing parameters and the performances of the superconducting core of the ceramic–metal composite conductor is necessary.

Previous work dealing with $(Bi, Pb)_2Sr_2Ca_2Cu_3O_{10}$/Ag tapes has demonstrated that hard x-rays are a valuable probe for studying *in situ* the phase transformations and microstructure evolution occurring during heat treatment in a ceramic that is clad inside a metal sheath [11–18]. Recently, Baranov *et al* [19] used synchrotron radiation to study the formation of MgB_2 under pressure from various precursor powder mixtures containing Mg and B or BN. They found a dependence between the applied pressure and the temperature at which the MgB_2 phase starts forming.

We performed *in situ* investigations of phase development inside Fe-sheathed wires under normal pressure. The formation of MgB_2 and MgO as well as the progress of the ceramic–sheath interface reaction can be followed during the heat treatment without the need for removing the sheath material, in spite of the strong diffraction contribution resulting from the presence of Fe.

2. Experimental details

Commercial Mg (average particle size ≈30 μm, 99.8% purity) and B (≈1 μm, amorphous, 90% purity, Mg content 5%) powders from Alfa Aesar were mixed in the appropriate ratio and homogenized by ball milling for 10 min. The powder was packed in an Fe tube (outer diameter 4.5 mm, wall thickness 0.75 mm), which was then deformed by rotary swaging followed by two-axial rolling into rectangular wires of 1.24 mm × 1.24 mm cross-section.

The measurements were conducted at the DESY-HASYLAB synchrotron facility on beamline BW5 with a 90 keV incident beam. Details on the experimental set-up and data analysis may be found in a previous publication [12]. Short pieces of wires (2 cm length) were clamped in a steel holder inserted in a quartz tube. The sample holder assembly was placed in a high-temperature furnace equipped with Kapton windows and a stainless steel heat shield with holes for beam entrance and exit. The samples were maintained in a flow of Ar ($\leqslant$0.5 ppm residual O_2) during the runs. Small pieces of Ta foil were placed in the bottom part of the sample space to act as an oxygen getter. A heating rate of 200 °C h^{-1} was used to reach the annealing temperature. A thermometer was situated close to the samples and the temperature was stable within 0.5 °C for 3 h long dwells at annealing temperatures of 650, 700 and 780 °C respectively. Previous studies on wires from the same preparation batch showed that the T_c of the MgB_2 phase (37.5 $\pm$ 0.5 K) and the normalized resistance of the wires are not affected by the heat treatment temperature in this range [20]. However, the absolute value of the normal state resistivity of the wires increases slightly with the heat treatment temperature due to the formation of a thicker Fe_2B layer at the sheath–ceramic interface [21].

A beam cross-section of 1 × 1 mm^2 was chosen to probe the ceramic core throughout the diameter of the wire. Absorption scans were used to position the samples in the beam. Diffraction patterns were recorded on a two-dimensional image plate and evaluated using the fit2d software package [22]. The intensity of the signal was normalized to the x-ray beam current value, which varies with time during the experiment.

3. Results and discussion

3.1. MgO formation

As shown in figure 1 for the run at 700 °C, the intensity of the Mg diffraction lines is already decreasing during the heating stage at low temperatures. This decrease is partly due to enhanced lattice vibrations and may be accounted for by use of the Debye–Waller factor determined by Haskel *et al* [23]. The corrected values are plotted versus temperature in the inset of figure 1. Up to $T \approx 100$ °C, the intensity of the Mg reflections is nearly constant within the experimental accuracy, but above this value, a clear linear decrease is observed, which most probably results from a chemical process. The rate of crystalline Mg disappearance accelerates significantly around $T = 450$ °C and at $T \approx 650$ °C, the intensity of the Mg diffraction lines suddenly vanishes, as expected from the melting point of the metal (651 °C).

The vapour pressure of Mg is relatively high even in the solid state, but it is not high enough to account for the progressive disappearance of the phase below its melting temperature (1–3 mm Hg at 651 °C [24]). Evaporation through the open ends of the wire cannot be completely ruled out but it is not expected to be the main reason for the disappearance of Mg. In fact, under constant temperature conditions, slow Mg evaporation only occurs above 400–550 °C [25–28] under 1 atm of Ar, N_2 air or O_2 (350 °C in high vacuum [29, 30]), whereas we observe that Mg is already starting to disappear

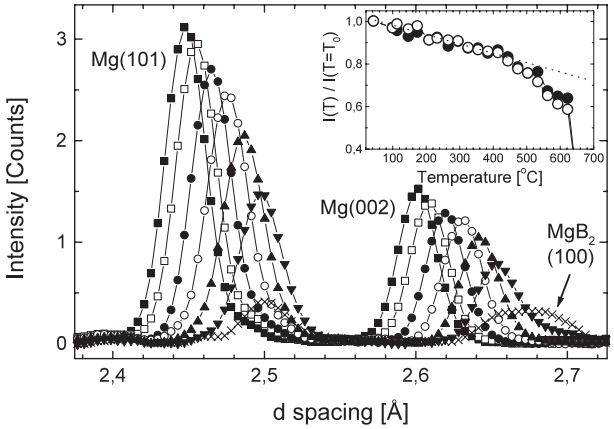

Figure 1. Evolution of the (101) and (002) reflections of Mg as a function of temperature during heating for the sample annealed at 700 °C. Patterns recorded at (from left to right): ■, 43 °C; □, 147 °C; ●, 266 °C; ○, 384 °C; ▲, 503 °C; ▼, 622 °C; ×, 652 °C. Inset: normalized integrated intensity: ○, (101); ●, (002). The dotted line is a guide to the eye. The standard deviation on the intensity values is approximately 1%, i.e. smaller than the symbol size.

from at least 100 °C during a heating ramp with a rate of 200 °C h^{-1}.

Since metallic Mg is prone to oxidation, even in the presence of very low oxygen partial pressures, the formation of MgO might explain the decreasing intensity of the Mg diffraction lines. However, detecting MgO in diffraction patterns is not an easy task in the present system, because of the very few diffraction lines accessible within the angular range covered by the experimental set-up, i.e. (111), (200), (220), (311) and (222) suffer from overlap with more intense peaks from other phases. The most intense diffraction peaks of MgO(200) and MgB_2(101) are nearly overlapping with room temperature d-spacings of 2.106 and 2.128 Å respectively. At this position, a faint peak is observed even prior to heat treatment. The intensity of this peak is plotted as a function of temperature in figure 2. It starts to increase significantly from $T = 575 \pm 15$ °C. The position of the peak follows a linear displacement towards larger d-spacing values up to $T \approx 575$ °C at a rate corresponding to the thermal expansion of MgO. However, above this temperature, the centre of mass of the peak departs from a linear thermal expansion behaviour and reaches values close to the expected position for the (101) reflection of MgB_2. Therefore, it is concluded that the phase forming at $T \geqslant 575$ °C during the heating ramp is MgB_2. Checking the intensity evolution of other MgB_2 reflections that have a lower relative intensity but are free from overlap, we confirm that extended MgB_2 formation starts around 575 °C. This reaction contributes therefore to the consumption of Mg below 650 °C. On the other hand, it appears that a small amount of MgO was already present in the starting powder. The intensity of the (200) reflection of MgO is difficult to follow at $T \leqslant 500$ °C, because it lies in the tail of a large Fe diffraction line, which induces a relatively high background at its position.

The second most intense MgO reflection ((220), relative intensity ≈50%) overlaps with the (103) reflection of Mg. Accordingly, its intensity cannot be followed independently

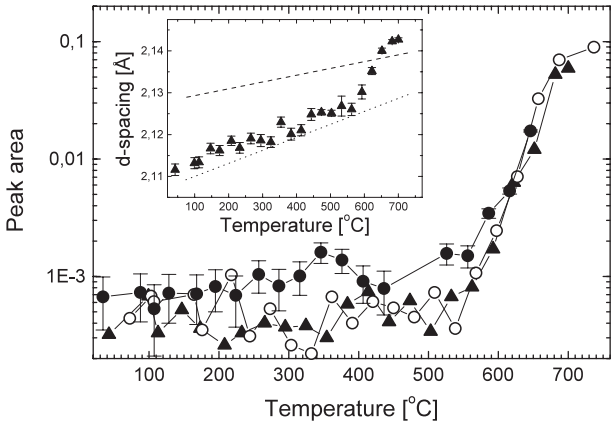

Figure 2. Integrated intensity of combined MgO(200) and MgB_2(101) reflections as a function of temperature during the heating stage for samples annealed at: ●, 650 °C; ▲, 700 °C; and ○, 780 °C. For clarity, standard deviations have been indicated for one sample only. Inset: position of the centre of the diffraction peak versus temperature (sample annealed at 700 °C). Dotted line: calculated *d*-spacing value of the MgO(200) reflection using the thermal expansion coefficient from [31]; dashed line: calculated *d*-spacing value of the MgB_2(101) reflection using the thermal expansion coefficient from [32].

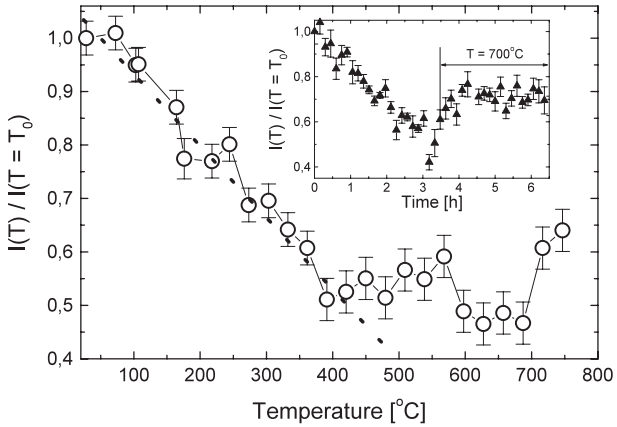

Figure 3. Normalized integrated intensity of the convolution of the Mg(103) and MgO(220) reflections versus temperature during the heating stage at 200 °C h^{-1} (sample annealed at 780 °C). Inset: similar data for the sample annealed at 700 °C but versus total heat treatment time.

during the heating stage. However, as evidenced in figure 3, a plot of the normalized intensity versus temperature of the convolution of these two reflections shows a departure from a linear decrease at a temperature close to 450 °C. The intensity does not reach zero even above the melting temperature of Mg. This is in contrast with the behaviour of all other observable Mg reflections and indicates that the MgO(220) reflection contribution to the integrated intensity becomes more and more significant from $T \approx 450$ °C, which in turn corresponds to the enhanced Mg consumption rate as observed using non-overlapping Mg reflections (figure 1). The sharp intensity drop around 600 °C in figure 3 may be attributed to the increased Mg consumption rate due to MgB_2 formation and melting of the remaining solid Mg, whereas the increase above 700 °C probably reflects the continuing formation of MgO after all the solid Mg has disappeared. This observation shows that MgO forms at lower temperatures than MgB_2 ($T = 450$ °C versus 575 °C) during the heating ramp used for reaching the reaction–sintering temperature of MgB_2-based wires and suggests that Mg oxidation plays a significant role in the progressive disappearance of Mg. The above data cannot however explain the decrease of the Mg intensities at $T \leqslant 450$ °C, because the integrated intensity of the (103) reflection of Mg decreases at the same rate as the intensity of all other observable Mg reflections. In fact, if crystalline MgO was forming at $T < 400$ °C, one would expect a lower apparent rate for the decrease of the Mg(103) reflection.

Studying the surface oxidation of Mg single crystals in air from room temperature to 400 °C, Fournier *et al* [26] observed that a very thin MgO layer is already forming at room temperature. The thickness of this layer increases with temperature and amounts to 4.3 nm after annealing at 400 °C for 15 min only. These authors also report a roughening of the MgO surface layer at 400 °C. Furthermore, a change in the oxidation kinetics of Mg has been observed by Gol'dshleger and Amosov [27] around 560 °C for an atmosphere containing 1.2% O_2 in Ar.

A direct comparison of these results with our observations is difficult due to the large difference in experimental conditions. According to observations performed by scanning electron microscopy on a polished cross-section of an unreacted wire, the average grain size of the initial Mg particles is approximately 15 μm, with an aspect ratio between 2 and 10. The formation of a 4 nm MgO layer on the surface of grains with such a size would hardly account for more than 0.2% of the Mg consumption. However, the observations of Fournier *et al* [26] were performed on the surface of polished single crystals. After mechanical deformation, the surface of the Mg particles inside the wires is rough, resulting in an enhanced surface area, which should allow for a more extensive oxidation. An x-ray diffraction line profile analysis by means of the integral breadth method was carried out to estimate the coherent domain size of the Mg particles in the as-deformed wires, using the relation

$$\beta = 2\varepsilon \tan\theta + \frac{\lambda}{d\cos\theta}$$

where β is the integral breadth, ε is the strain, θ the Bragg scattering angle, λ the x-ray wavelength and d the average grain size of the coherent crystalline domains [33]. A value of 45 ± 5 nm, independent of the crystallographic orientation, was found. If oxygen can diffuse to some extent along coherent domain boundaries within the macroscopic grains, a large amount of Mg might be converted to MgO during the heating ramp.

MgO layers of a few nanometres' thickness cannot be detected by our experimental technique. From 400 °C [26] or 550 °C [27], slow evaporation of Mg is reported to result in a significant increase of the oxidation kinetics of Mg. If a similar effect is at play in our wires, it would explain the accelerating rate of the Mg disappearance and the detection of MgO from $T \approx 450$ °C.

The residual oxygen partial pressure in the Ar gas used for the present experiments (0.5 ppm) is much lower than that for the aforementioned studies on Mg oxidation [26, 27].

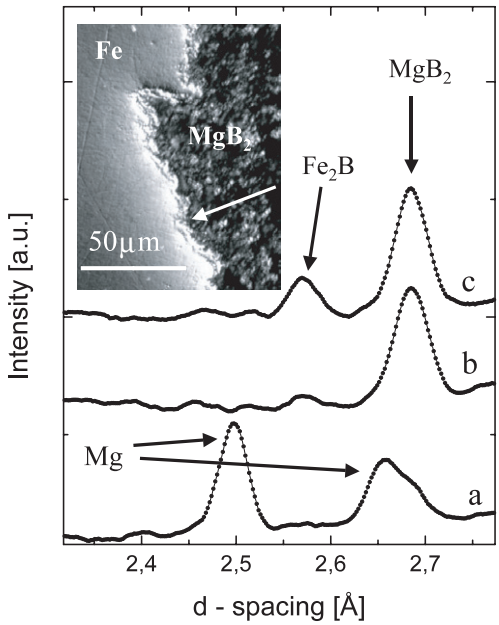

Figure 4. Selected diffraction patterns showing the appearance and evolution of the Fe_2B phase: (a) 657 °C; (b) 780 °C, 10 min; (c) 780 °C, 2 h 30 min. Inset: optical micrograph showing the Fe_2B interface layer formed after 3 h 20 min at 780 °C (transverse polished cross-section).

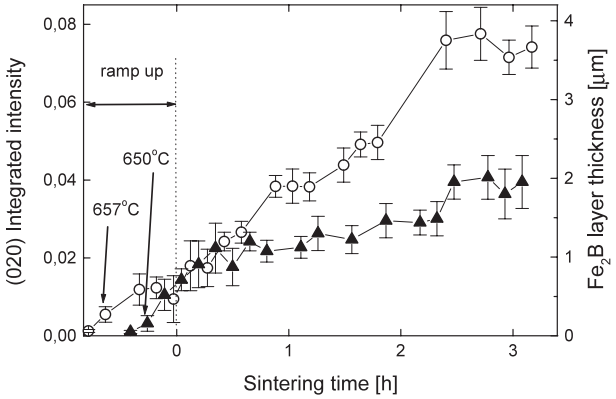

Figure 5. Evolution of the Fe_2B phase content during annealing at, ▲, 700 °C and, ○, 780 °C. The thickness is obtained by calibration with microscopic observations performed on polished cross-sections of the same samples after completion of the heat treatment.

Furthermore, the Ta foil pieces added in the sample space close to the wires as well as the Fe sheath itself absorb a part of the residual oxygen as evidenced by a thin oxide layer formed on the surface of the wires and the Ta pieces. Kováč *et al* [34] already reported that a 30 min heat treatment at 950 °C in an argon atmosphere results in a non-negligible increase of the MgO phase content in wires prepared from pre-reacted MgB_2 powders. While it cannot be ruled out that residual oxygen in the argon atmosphere surrounding the samples may contribute to the formation of MgO, it is also possible that oxygen is already present inside the samples in relatively large amounts prior to the start of the heat treatment. According to Eyidi *et al* [35], large amounts of oxygen (up to 10%) can be found even in wires heat treated in a reducing atmosphere of Ar/H_2 (5%). Oxygen might be incorporated in the samples to some extent during the preparation process when manipulations are performed in air. The Mg and B precursor powders are also likely to contain oxygen in the form of a thin surface corrosion layer, which is not necessarily detected by means of x-ray diffraction. We plan to perform similar studies under reducing or slightly oxidizing conditions in order to check for a possible influence of the Mg losses and MgO formation behaviour.

3.2. Fe_2B formation

It has been widely reported that a reaction layer forms during heat treatment at the Fe/MgB_2 interface in wires and tapes prepared both by the *in situ* [36–39] and the *ex situ* [40–45] preparation routes.

As illustrated in figure 4, Fe_2B was readily detected in our diffraction measurements. Figure 5 depicts the evolution of the (020) reflection of this phase for the wires heat treated at 700 and 780 °C. Once the sintering temperature has been reached, the increase of the Fe_2B scattering volume is linear to a first approximation. This indicates that the interface layer does not act as a diffusion barrier against further reaction between the sheath and the ceramic core, at least up to the thickness of the Fe_2B reaction layer formed during the present experiments. Comparing the Fe_2B layer thickness as observed by microscopy on polished cross-sections of the samples after the *in situ* runs (figure 4) with synchrotron data recorded for the same samples, it is possible to relate the intensity of the Fe_2B reflections to the actual thickness of the reaction layer. As appears from figure 5, the threshold thickness for detection of the Fe_2B corresponds approximately to 150–200 nm. It is noteworthy that thicker reaction layers have been formed on similar samples during a heat treatment of 30 min at 600–750 °C during independent experiments [20], showing that the fine details of the heat treatment schedule are likely to play a significant role in the development of the ceramic–metal interaction.

For both runs presented in figure 5, the Fe_2B phase is already forming during the heating ramp and is detected from $T = 655 \pm 5$ °C. In the third *in situ* run, for which a sintering temperature of 650 °C was maintained, the intensity of the Fe_2B reflection was not much higher than the intensity of the background noise during the 3 h spent at constant temperature. Figure 5 clearly illustrates that the use of lower heat treatment temperatures reduces the formation rate of Fe_2B. However, other parameters, like the average particle size of the precursor powders, can have a strong influence on the interface reaction conditions. For instance, Fisher *et al* [37] reported that a 0.5 μm thin reaction layer formed after 3 h sintering at 500 °C when mechanically alloyed nanometre-sized precursors were used.

In samples prepared from pre-reacted MgB_2 (*ex situ* route), the formation of Fe_2B occurs either through a direct reaction between Fe and MgB_2 or via a reaction between Fe and decomposition products of MgB_2. The interface reaction layer typically forms at $T \geqslant 800$ °C [40–45]. Some authors even report no extended Fe_2B formation up to 900 °C [46, 47]. We can therefore reasonably expect that the MgB_2 formed during our investigations does not react with the sheath during the 3 h sintering periods, at least up to 700 °C.

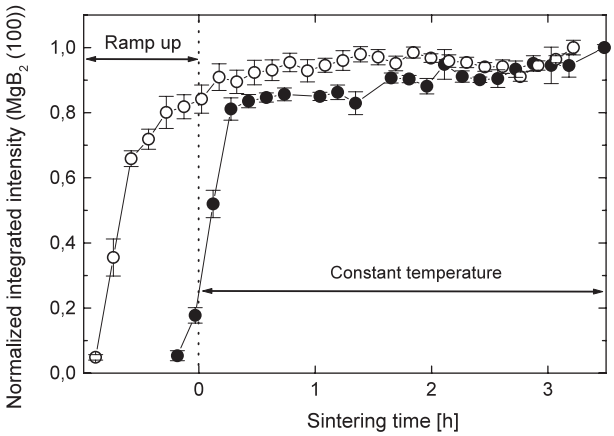

Figure 6. Evolution of the MgB_2 phase content based on the integrated intensity of the (100) reflection normalized to the intensity reached at the end of the high-temperature sintering period. ●, 650 °C; and ○, 780 °C.

3.3. MgB_2 formation

Figure 6 shows the time dependence of the MgB_2(100) reflection intensity for the samples heated to 650 and 780 °C. A similar behaviour was observed for the wire heated to 700 °C. Most of the MgB_2 phase forms during the end of the heating ramp and the first half hour at the annealing temperature. Afterwards, only a slight intensity increase is observed. The MgB_2 volume does not appear to decrease with time, even for a 3 h heat treatment at 780 °C, where a significant amount of Fe_2B forms. This further suggests that, under the present experimental conditions, the Fe_2B phase does not result from a direct reaction between MgB_2 and the Fe sheath. It is more likely that the Fe reacts with the unreacted B powder, which could not react with the Mg trapped as MgO. MgO was also detected in the wire annealed at 650 °C, but the Fe–B reaction is probably too slow at this temperature to result in a significant amount of Fe_2B within 3 h. Mg oxidation and MgB_2 formation can be considered as two concurrent reactions. As long as the temperature is low enough to avoid a reaction between the Fe sheath and MgB_2 or its decomposition products, avoiding the formation of MgO would in principle help in preventing the formation of Fe_2B by trapping B into the MgB_2 phase.

As reported above, the MgB_2 phase was found to form from about 575 °C, i.e. during the heating ramp. Since the heating rate was 200 °C h^{-1}, it is likely that the reaction between Mg and B started at a significantly lower temperature but with slower formation kinetics, in agreement with independent measurements on samples from the same batch [20].

4. Summary and conclusions

The intensity of the Mg reflections significantly decreases during the heating stage from temperatures as low as 100 °C. The formation of MgO is evidenced from 450 °C and is probably the major factor causing the Mg disappearance during the heating stage up to 575 °C. The origin of the oxygen responsible for this effect is not clear. The inclusion of MgO nanoparticles in MgB_2 grains has been related to enhanced flux pinning capability [48] and the formation of MgO in the MgB_2 matrix may therefore be considered as an advantage. However, mastering this structural feature will require a thorough understanding of the MgO formation mechanism and a control of the oxygen source(s).

Extended MgB_2 phase formation occurs from 575 °C, i.e. below the melting point of metallic Mg. However, MgB_2 starts forming at higher temperatures than the MgO phase, which in turn could hamper the reaction leading to the formation of MgB_2.

Formation of Fe_2B was detected in the samples heat treated at 700 and 780 °C, but not those heat treated at 650 °C. Its formation appears to result from a direct interaction between the Fe sheath and elemental boron. The increase of the Fe_2B layer thickness is linear to a first approximation, showing that the interfacial layer does not act as a diffusion barrier against further reaction between the sheath and the ceramic core. The detection limit for Fe_2B corresponds to a layer thickness of 150–200 nm, making diffraction by hard x-rays a very interesting tool for the non-destructive, room temperature examination of the interface reaction in longer Fe-sheathed MgB_2 wires and tapes after heat treatment.

Acknowledgments

This work was supported by the Danish Technical Research Council under the Framework Programme on Superconductivity and by the European Union under the Framework Programme FP6 (project ‘HIPERMAG’, contract No 505724-1).

References

[1] Nagamatsu J, Nakagawa N, Muranaka T, Zenitani Y and Akimitsu J 2001 *Nature* **410** 63
[2] Grasso G, Malagoli A, Ferdeghini C, Roncallo S, Bracini V and Siri A 2001 *Appl. Phys. Lett.* **79** 230
[3] Suo H L, Beneduce C, Dhallé M, Musolino N, Genoud J-Y and Flükiger R 2001 *Appl. Phys. Lett.* **79** 3116
[4] Glowacki B A, Majoros M, Vickers M, Evetts J E, Shi Y and McDougall I 2001 *Supercond. Sci. Technol.* **14** 193
[5] Jin S, Mavoori H, Bower C and van Dover R B 2001 *Nature* **411** 563
[6] Soltanian S *et al* 2001 *Physica* C **361** 84
[7] Goldacker W, Schlachter S I, Zimmer S and Reiner H 2001 *Supercond. Sci. Technol.* **14** 787
[8] Pradhan A K, Feng Y, Zhao Y, Koshizuka N, Zhou L, Zhang P X, Liu X H, Ji P, Du S J and Liu C F 2001 *Appl. Phys. Lett.* **79** 1649
[9] Kumakura H, Matsumoto A, Fujii H and Togano K 2001 *Appl. Phys. Lett.* **79** 2435
[10] Scanlan R M, Malozemoff A P and Larbalestier D C 2004 *Proc. IEEE* **92** 1639
[11] Thurston T R, Wildgruber U, Jisrawi N, Haldar P, Suenaga M and Wang Y L 1996 *J. Appl. Phys.* **79** 3122
[12] Poulsen H F, Frello T, Andersen N H, Bentzon M D and Zimmermann M v 1998 *Physica* C **298** 265
[13] Jiang J, Shields T C, Abell J S and Bushnell-Wye G 1998 *Physica* C **306** 91
[14] Poulsen H F, Andersen L G, Frello T, Prantontep S, Andersen N H, Garbe S, Madsen J, Abrahamsen A, Bentzon M D and Zimmermann M v 1999 *Physica* C **315** 254
[15] Frello T, Poulsen H F, Andersen L G, Andersen N H, Bentzon M D and Schmidberger J 1999 *Supercond. Sci. Technol.* **12** 293

[16] Maroni V A, Venkataraman K, Kropf A J, Segre C U, Huang Y and Riley G N 2002 *Physica* C **382** 21
[17] Chen X P, Han Z, Grivel J-C, Xu G J, Andersen N H and Homeyer J 2005 *J. Mater. Sci.* **40** 213
[18] Grivel J-C, Raittila J, Xu G J, Chen X P, Han Z, Homeyer J and Andersen N H 2005 *Supercond. Sci. Technol.* **18** 583
[19] Baranov A N, Solozhenko V L, Lathe C, Turkevich V Z and Park Y W 2003 *Supercond. Sci. Technol.* **16** 1147
[20] Kováč P, Hušek I, Melišek T and Štrbík V 2005 *Supercond. Sci. Technol.* **18** 856
[21] Kováč P, Hušek I and Melišek T 2005 unpublished result
[22] Hammersley A P, Svensson S O, Hanfland M, Fitch A N and Häusermann D 1996 *High Pressure Res.* **14** 235
[23] Haskel D, Sarikaya M, Qian M and Stern E A 1995 *Ultramicroscopy* **58** 353
[24] *Gmelin Handbuch der anorganischen Chemie* 1972 vol 27, part A (Weinheim: Chemie GMBH) p 221
[25] Dupre B and Streiff R 1972 *J. Nucl. Mater.* **42** 260
[26] Fournier V, Marcus P and Olefjord I 2002 *Surf. Interface Anal.* **34** 494
[27] Gol'dshleger U I and Amosov S D 2004 *Combust. Expl. Shock Waves* **40** 275
[28] Grall L 1955 *Rev. Metall.* **52** 603
[29] Bronfin M B, Zhukhovitskii A A and Marichev V A 1966 *Sov. Phys.—Solid State* **7** 2107
[30] Tatus V I, Kolot V Ya, Fogel' Ya M, Bokshteyn S Z and Bronfin M B 1974 *Rus. Metall.* **6** 84
[31] Fang M X, Te P and Yan Z T 2004 *Phys. Status Solidi* b **241** 2464
[32] Jorgensen J D, Hinks D G and Short S 2001 *Phys. Rev.* B **63** 224522
[33] Williamson G K and Hall W H 1953 *Acta Metall.* **1** 22
[34] Kováč P, Hušek I, Melišek T, Grivel J-C, Pachla W, Štrbík V, Diduszko R, Homeyer J and Andersen N H 2004 *Supercond. Sci. Technol.* **17** L41
[35] Eyidi D, Eibl O, Wenzel T, Nickel K G, Schlachter S I and Goldacker W 2003 *Supercond. Sci. Technol.* **16** 778
[36] Fu B Q, Feng Y, Yan G, Liu C F, Zhou L, Cao L Z, Ruan K R and Li X G 2003 *Physica* C **392–396** 1035
[37] Fischer C, Hässler W, Rodig C, Perner O, Behr G, Schubert M, Nenkov K, Eckert J, Holzapfel B and Schultz L 2004 *Physica* C **406** 121
[38] Goldacker W, Schlachter S I, Obst B, Liu B, Reiner J and Zimmer S 2004 *Supercond. Sci. Technol.* **17** S363
[39] Xu H L, Feng Y, Xu Z, Li C S, Yan G, Mossang E and Sulpice A 2005 *Physica* C **419** 94
[40] Kováč P, Hušek I and Melišek T 2002 *Supercond. Sci. Technol.* **15** 1340
[41] Yamamoto K, Osamura K, Balamurugan S, Nakamura T, Hoshino T and Muta I 2003 *Supercond. Sci. Technol.* **16** 1052
[42] Grovenor C R M, Goodsir L, Salter C J, Kováč P and Hušek I 2004 *Supercond. Sci. Technol.* **17** 479
[43] Pachla W, Presz A, Kováč P, Hušek I and Diduszko R 2004 *Supercond. Sci. Technol.* **17** 1289
[44] Balamurugan S, Nakamura T, Osamura K, Muta I and Hoshino T 2994 *Mod. Phys. Lett.* B **18** 791
[45] Lezza P, Gladyshevskii R, Suo H L and Flükiger R 2005 *Supercond. Sci. Technol.* **18** 753
[46] Serquis A, Civale L, Hammon D L, Coulter J Y, Liao X Z, Zhu Y T, Peterson D E and Mueller F M 2003 *Appl. Phys. Lett.* **82** 1754
[47] Song K J *et al* 2002 *Physica* C **370** 21
[48] Serquis A *et al* 2002 *J. Appl. Phys.* **92** 351